

A SEQUENTIAL LOCAL ENUMERATION-BASED IMPROVED LATIN HYPERCUBE SAMPLING METHOD FOR BALLISTIC CONSTRAINT DESIGN SPACE

Han Zeng^{1,2}, Zhong-Hua Han^{1,2,*}, Chen-Zhou Xu^{1,2}, Yang Zhang^{1,2}

¹Institute of Aerodynamic and Multidisciplinary Design Optimization, School of Aeronautics, Northwestern Polytechnical University, Xi'an, 710072, China

²National Key Laboratory of Aircraft Configuration Design, Xi'an, 710072, China

Abstract

The design and optimization of complex aircraft usually requires thousands to tens of thousands of numerical simulations to complete, a costly process. Surrogate models have been widely used in engineering problems due to their feature of replacing complex and time-consuming numerical simulations. Design of experiment (DoE) is an important and indispensable part of the process of establishing a surrogate model, and its sampling results have a crucial impact on the accuracy of the model and the subsequent optimal design. Existing DoE methods such as Latin hypercube sampling (LHS) are mainly targeted at unconstrained design space. But in actual engineering problems, such as the ballistic constrained design space in aircraft design is often subject to multiple and strong constraints on the ballistic trajectory, and then the unconstrained DoE method is no longer applicable. The constrained DoE method: sequential local enumeration-based Latin hypercube sampling for constrained design space (SLE-CLHS) for the constraint space is unable to establish the constraints of the ballistic constraint design space of the whole vehicle. Therefore, based on SLE-CLHS, this paper proposes a sequential local enumeration-based improved Latin hypercube sampling method for ballistic constraint design space (BCDS-ILHS), which ensures better exploration of the design space by establishing the constraints of the ballistic trajectory, improves the correctness and accuracy of the sampling, and establishes a higher accuracy surrogate model with as few samples as possible. In order to verify the feasibility of the proposed BCDS-ILHS in the ballistic constraint design space, we apply it to a 3D numerical case and a 3D engineering case. The results show that BCDS-ILHS is able to generate samples that satisfy the constraints compared to LHS. And in most cases, with the same prediction accuracy of the surrogate model, BCDS-ILHS requires fewer samples.

Keywords: Design of experiment; Latin hypercube sampling; Ballistic constraint; Surrogate model

1. General Introduction

In the design and optimization of complex aircraft, thousands to tens of thousands of numerical simulations are usually required, a costly process. Surrogate models, also known as approximate models or meta-models, have been widely used in engineering problems due to their characteristic of replacing complex and time-consuming numerical simulations [1]. Design of experiment (DoE) is an indispensable and important part of the process of establishing a surrogate model, and its sampling results have a crucial impact on the accuracy of the model and the subsequent optimal design [2]. Existing DoE methods mainly include Latin hypercube sampling (LHS) [3], Hammersley sequence sampling (HSS) [4], orthogonal design (OD) [5], uniform design (UD) [6], and central composite design (CCD) [7], etc., among which, LHS is one of the most popular DoE methods. The projections of any two samples in any dimension in LHS will not overlap, which can reduce

unnecessary tests in the same dimension, and has been widely used in the optimization design of airfoils [8], wings [9] and helicopter rotor blades [10], etc. The above mentioned DoE methods can only be used in the unconstrained design space. In actual engineering problems, the design space is often multi-constrained and strongly constrained, when the unconstrained DoE method is no longer applicable. Therefore, under the condition of considering constraints, Petelet [11] proposed a LHS method considering inequality constraints, where the initial LHS is replaced according to the desired monotonic constraints, but the space-filling property of the samples deteriorates when the maximum or minimum bounds of the two constrained variables are close to each other. Trosset [12] constructed an approximate maximum and minimum DoE method for constrained design spaces by using nonlinear programming and the L_p criterion. But as the constraints increase, the problem size increases drastically, which leads to a reduction in the efficiency of the DoE. Stinstra [13] proposed a sequential method (SFDP**) for solving maximum and minimum DoE problems for constrained design spaces. And relative to the method proposed by Trosset, the SFDP**'s problem size is insensitive to the number of DoE and constraints between variables and has high efficiency. But the projection properties of the samples are poor. Danel [14] proposed a constrained non-collapsing design (CoNcaD), which can deal with any type of constraints. But the projection properties of the samples deteriorate as the problem dimensions become higher. Fuerle [15] minimized the problem size of the DoE by using the permutation genetic algorithm to minimize the points of the Audze-Eglais potential to find the optimal Latin hypercube (OLH). And then combining the constraints to extend the OLH to the constrained design space. But when the number of samples becomes too large, the space-filling and projection properties of the samples deteriorate. Du [16] proposed a sequential local enumeration-based Latin hypercube sampling for constrained design space (SLE-CLHS) and applied it to rotor optimization of UAVs. SLE-CLHS directly establishes the constrained design space by considering the constraints between variables. The initial samples are firstly generated in the unconstrained design space by LHS. Then the samples that do not satisfy the constraints are eliminated. Finally, a line search is performed in the constrained design space to generate new samples, which need to satisfy the space-filling property and projection property of the overall sampling. The difficulty of this method is that it needs to establish the constraints of the whole design space, which is difficult or even impossible to be applied to complex engineering problems, such as the ballistic design space with multiple constraints and strong constraints. Therefore, based on SLE-CLHS, this paper proposes a sequential local enumeration-based improved Latin hypercube sampling method for ballistic constraint design space (BCDS-ILHS) to solve the DoE problem of ballistic constraint design space, which avoids establishing constraints of the whole design space by constraining points on the ballistic trajectory individually. And at the same time, BCDS-ILHS ensures that the samples strictly satisfy the constraints in the conditions, the design space is better explored and the sampling correctness and accuracy are improved.

The remainder of this paper is organized as follows. In Section 2, the specific sampling steps of BCDS-ILHS are introduced, as well as the numerical simulation method and the surrogate model used in this paper. In Section 3, BCDS-ILHS is applied to a 3D numerical case and a 3D engineering case, and the results are presented. In Section 4, the conclusions are presented.

2. Methodology

2.1 BCDS-ILHS

Aiming at the DoE problem of the ballistic constraint design space, BCDS-ILHS ensures that the design space can be better explored and the correctness and accuracy of the sampling can be improved by establishing the constraints of the ballistics under the condition that the samples strictly satisfy the constraints. Specifically, for a n-dimensional ballistic constraint design space, the algorithm steps are as follows:

- (1) Given ballistic data (usually consisting of a series of discrete points) and interpolating it to obtain a continuous trajectory.
- (2) Establish a constraint equation based on the constraints of the trajectory, with the constraint that the Euclidean distance between the sample to be sampled and a point on the trajectory at the same altitude segment is not greater than a given value, R.
- (3) The LHS is used to generate m samples in the design space without ballistic constraints, of which there are t samples that satisfy the constraint equations, $t \le m$. Therefore, after eliminating the samples that do not satisfy the constraints, the number of samples that need to be added is m-t.
- (4) Select one of the n dimensions as the base dimension, denoted as \dim_1 . Arrange these t samples from smallest to largest value in the \dim_1 dimension, denoted as $X = \{x_1, x_2, \cdots, x_t\}$. And compute the distance between neighboring points in the \dim_1 dimension, denoted as $D = \{d_1, d_2, \cdots, d_{t+1}\}$.
- (5) Select the two neighboring points in X that have the largest distance in the \dim_1 dimension, give the value of the t+1 sample to be supplemented in the \dim_1 dimension at 1/2 of these two points, and update D.
- (6) Select one of the n dimensions as the \dim_2 dimension, and given that the search step of this dimension is λ_{\dim_2} , search the t+1 sample in the \dim_2 dimension. Because the value in the \dim_1 dimension has already been determined, this search is mainly to determine the value of the t+1 sample in the \dim_2 dimension. Search from the lower bound of the constraint to the upper bound of the constraint with the step λ_{\dim_2} in \dim_2 dimension. In the search process, calculate the Euclidean distance between the to-be-sampled point and the sampled point according to the formula (1), and select the position where the Euclidean distance is the largest as the value of the t+1 sample in \dim_2 dimension. Repeat the above process until the value of the t+1 sample in all dimensions is recognized. At this time, $X_{new} = \{x_1, x_2, \cdots, x_t, x_{t+1}\}$.
- (7) Repeat steps (5)~(6) until the number of samples in X reaches m, and sampling ends.

Euclidean Distance =
$$\sqrt{\sum_{i=1}^{\dim_x} (x_a^i - x_0^i)^2}$$
 (1)

where \dim_x denotes the dimension in which the step search is being performed. x_a^i denotes the value of the a sample to be sampled in the i dimension. x_0^i denotes the value of sample in the X-sample set in the i dimension.

A simple 2D example is used here to simulate the DoE problem in ballistic constraint design space, which in turn demonstrates the BCDS-ILHS sampling steps in detail (as shown in Figure 1). The design space is

$$x_1, x_2 \in [0,1] \tag{2}$$

The trajectory is

$$x_2 = x_1^2$$
 (3)

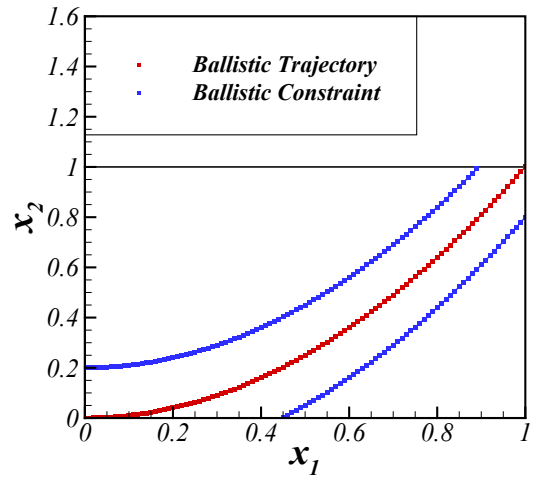
The ballistic constraints are

$$\sqrt{(x_2 - x_1^2)^2} \le 0.2 \tag{4}$$

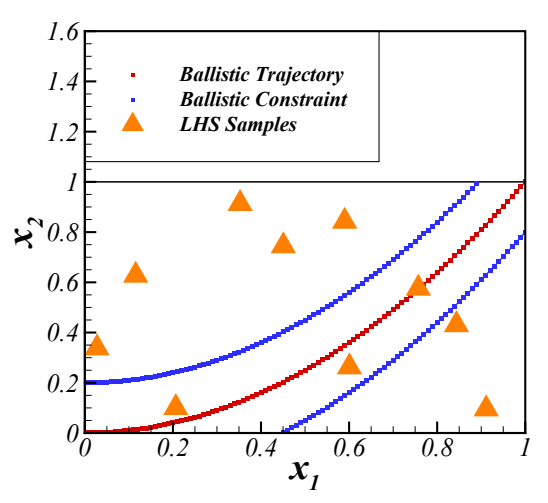
Selecting x_1 as the base dimension, the search step of BCDS-ILHS in x_2 dimension is

$$\lambda_{BCDS-ILHS} = 0.05 \tag{5}$$

The design space, ballistic trajectory and ballistic constraints are shown in Figure 1 (a). Firstly, 10 samples are sampled in the unconstrained design space by LHS (as shown in Figure 1 (b)). After eliminating the samples that do not satisfy the constraints, the remaining samples that satisfy the constraints are shown in Figure 1 (c). Next, taking x_1 as the base dimension, the remaining samples are arranged in order of their values in x_1 dimension from smallest to largest. The distance between neighboring points in x_1 dimension is calculated. The value of the first sample to be sampled in x_1 dimension is fixed at 1/2 of the largest distance between the neighboring points. Then, search from the lower bound of the constraint to the upper bound of the constraint in the x_2 dimension with the step λ_{r2} . In the searching process (as shown in Figure 1 (d)), the Euclidean distance between the samples to be collected and the existing samples is calculated. Finally, the sample with the largest Euclidean distance is selected to determine the value of the samples to be collected in the x_2 dimension, which determines the exact location of the samples to be collected in the ballistic constraint design space (as shown in Figure 1 (e)). The process of sampling subsequent samples is the same as the above, so it will not be repeated. The final sampling results are shown in Figure 1 (f). From the figure, it can be seen that the samples obtained by BCDS-ILHS strictly satisfy the constraints.



(a) Design space, ballistic trajectory, ballistic constraints



(b) Samples generated by LHS

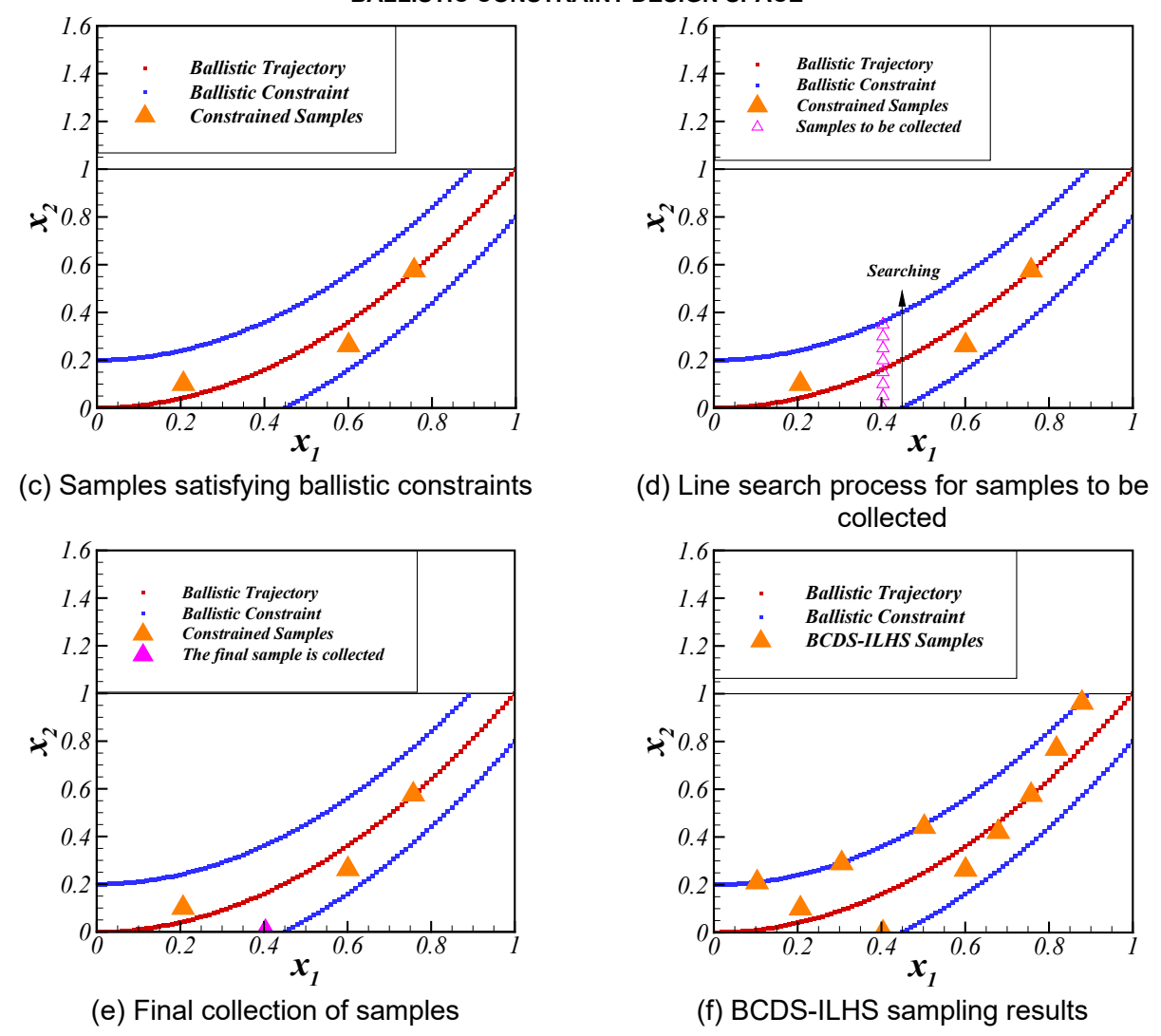


Figure 1 - Sampling process of BCDS-ILHS.

2.2 Numerical Simulation Methodology

In this paper, a Navier-Stokes equation-based solver is used for the flow solution, with Reynolds-averaged Navier-Stokes equations (RANS) as the flow control equations, AUSM format for the spatial discretization, and $k-\omega$ SST as the turbulence model of choice.

In order to verify the correctness and validity of the mesh generation method and numerical simulation method used in this paper, the aerodynamic characteristics of the FDL-5A [17] hypersonic vehicle (as shown in Figure 2) are computed at the Ma = 7.98, H = 24.5 km, $\alpha = 10^{\circ}$ state.



Figure 2 - FDL-5A hypersonic vehicle profile.

Boundary layer mesh is generated for the near-wall surfaces and tetrahedral mesh is generated for

the rest of the space, with a total of three sets of mesh, 48W, 100W, and 200W, as shown in Figure 3.

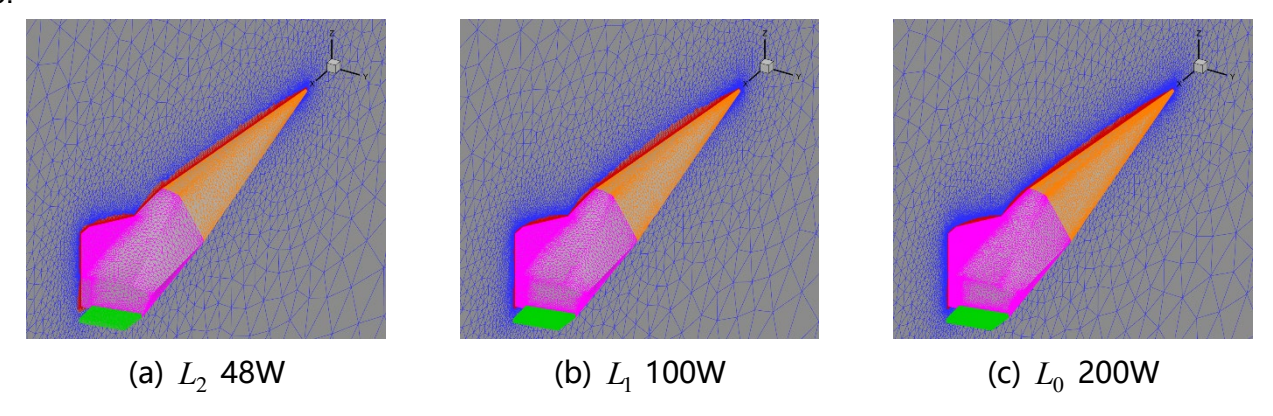


Figure 3 - FDL-5A hypersonic vehicle mesh.

The computational results are shown in Figure 4. The lift coefficients, drag coefficients and pitching moment coefficients at zero mesh spacing obtained by Richardson extrapolation [18] are also shown, from which it can be seen that the coefficients change approximately linearly with the amount of mesh. The mesh convergence is good, which verifies the correctness and validity of the mesh generation methodology and numerical simulation methodology used in this paper.

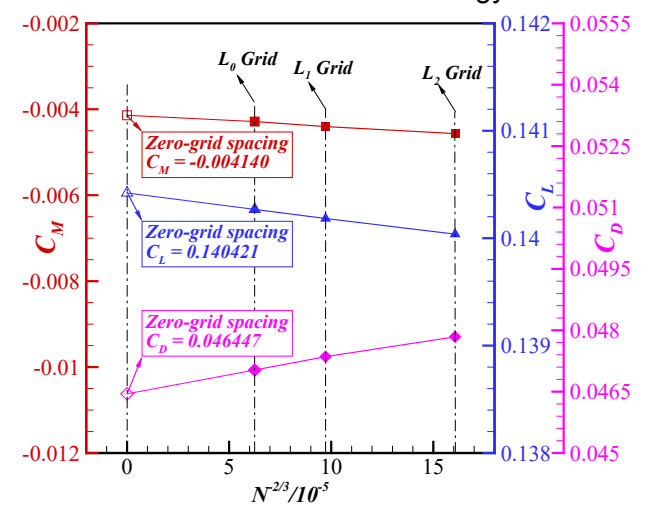


Figure 4 - FDL-5A hypersonic vehicle solver calculation results.

2.3 Surrogate Model

Surrogate model is an approximate mathematical model used to replace relatively complex and time-consuming numerical simulations in the design and optimization process. The Kriging [19-20], which has the ability to predict unknown points and error estimation, is a supervised machine learning model. In recent years, it has been widely applied in aerospace field, especially in modeling of aerodynamic data of small samples of vehicles.

The principle of the Kriging is to consider the unknown function as a concrete realization of some static random process. Specifically, for an arbitrary unknown position x, its corresponding function value y(x) is replaced by a random function Y(x), and y(x) is only a random result in Y(x), which is expressed as

$$Y(x) = \beta_0 + Z(x) \tag{6}$$

where β_0 is the mathematical expectation of Y(x), an unknown constant. And $Z(\cdot)$ is a static stochastic process with mean 0 and variance σ^2 .

The detailed modeling process of the Kriging can be found in the literature [1]. In this paper, the correlation function chosen in the modeling process is the "Gaussian quadratic exponential function", whose expression is as follows

$$R_k(\theta_k, x_k^{(i)} - x_k^{(j)}) = \exp(-\theta_k \left| x_k^{(i)} - x_k^{(j)} \right|^{p_k}), p_k = 2$$
(7)

where $x_k^{(i)}$ and $x_k^{(j)}$ are the k dimensional components of the i and j samples, respectively; θ_k is the model hyperparameters. When establishing the Kriging, in order to improve the accuracy of the model, it is usually necessary to train the hyperparameters of the model. In this paper, we use the maximum likelihood estimation for the hyperparameters to find the optimal. In addition, this paper uses statistical indicators to evaluate the accuracy of Kriging. The accuracy metrics are mainly coefficient of determination (R^2), relative root mean square error (RRMSE) and relative maximum absolute error (RMAE), where R^2 and RRMSE are the global accuracy metrics, and RMAE is the local accuracy metric, which are calculated as follows

$$R^{2} = 1 - \frac{\sum_{i=1}^{N} (y_{i} - \hat{y}_{i})^{2}}{\sum_{i=1}^{N} (y_{i} - \overline{y})^{2}}, R^{2} \in (-\infty, 1]$$
(8)

$$RRMSE = \frac{1}{STD} \sqrt{\frac{1}{N} \sum_{i=1}^{N} (y_i - \hat{y}_i)^2}$$
 (9)

$$RMAE = \frac{1}{STD} \max \left| y_i - \hat{y}_i \right| \tag{10}$$

$$STD = \sqrt{\frac{1}{N-1} \sum_{i=1}^{N} (y_i - \overline{y})^2}$$
 (11)

where N is the number of test samples, \hat{y}_i is the predicted value of the surrogate model at the i test sample, y_i is the true value of the test sample, \overline{y} is the average value of the true values of the test samples, and the closer R^2 is to 1, the smaller RRMSE and RMAE are, which indicates that the predictive accuracy of the surrogate model is higher.

3. Case Validation

3.1 Case 1: Three-dimensional Numerical Case

Taking the 3D Rastrigin analytic function f(x) as the modeling objective and x_1, x_2, x_3 as the variables, the DoE problem and the modeling problem in the ballistic constraint design space are simulated by sampling and building Kriging for f(x), and the analytic function expression is as follows

$$f(x) = 10 * 3 + \sum_{i=1}^{3} \left[x_i^2 - 10\cos(2\pi x_i) \right]$$
 (12)

The design space is

$$x_1, x_2 \in [-0.2, 1.2],$$

 $x_3 \in [0.0, 2.0]$ (13)

The trajectory is

$$x_3 = x_1^2 + x_2^2, x_1 = x_2 (14)$$

The ballistic constraints are

$$\sqrt{(x_1 - \sqrt{\frac{x_3}{2}})^2 + (x_2 - \sqrt{\frac{x_3}{2}})^2} \le 0.2$$
 (15)

 x_3 is selected as the baseline dimension, and the BCDS-ILHS search steps in the x_1, x_2 dimensions are all

$$\lambda_{BCDS-ILHS} = 0.001 \tag{16}$$

The design space, ballistic trajectory and ballistic constraints are shown in Figure 5. When the value of x_3 is determined, the ballistic constraints (blue circle) are shown in Figure 5 (a). and the complete ballistic constraints obtained from the ballistic trajectory are shown in Figure 5 (b) (gray pipe).

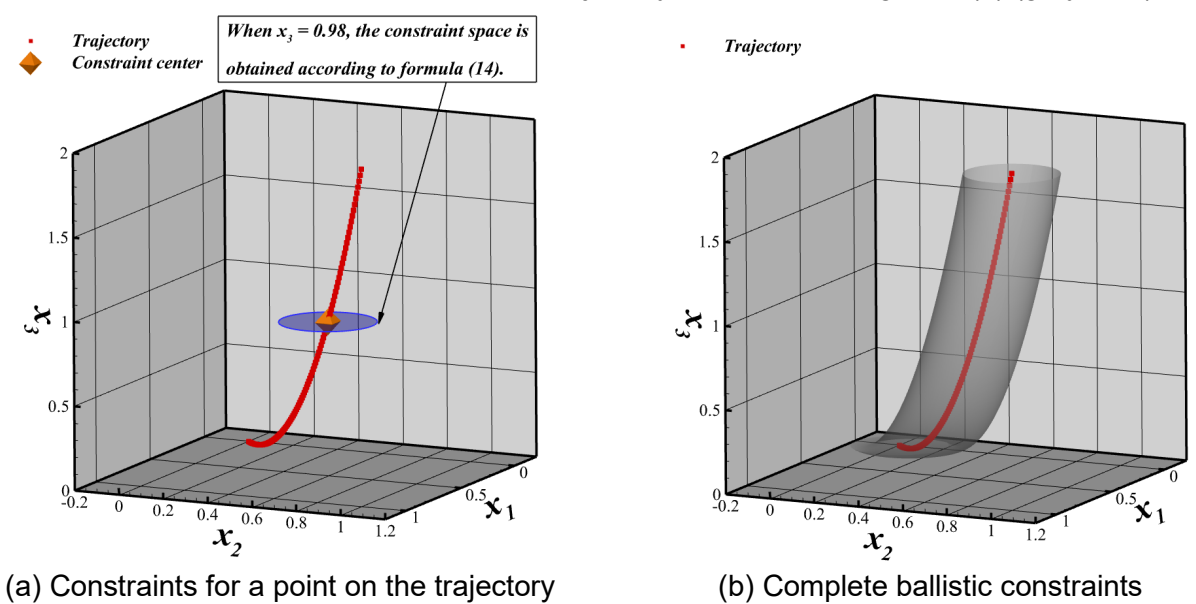
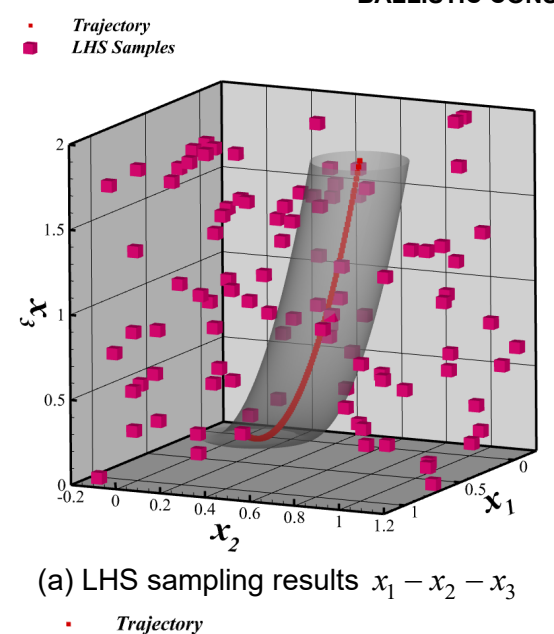
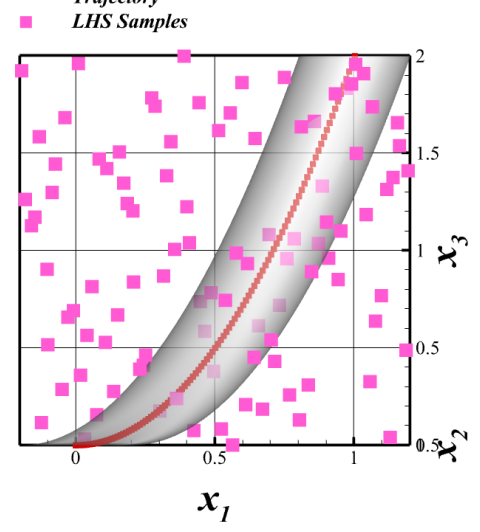


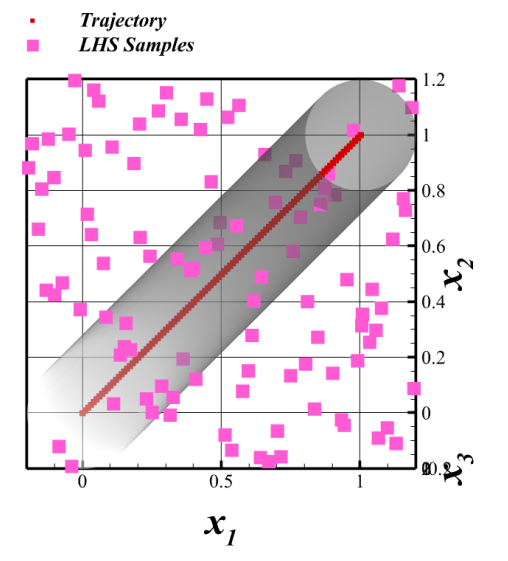
Figure 5 - 3D Rastrigin analytic functions for design space, ballistic trajectory, and ballistic constraints.

The LHS and BCDS-ILHS is used to sample the above design space with a sample size of 100 and the sampling results are shown in Figure 6 and Figure 7.

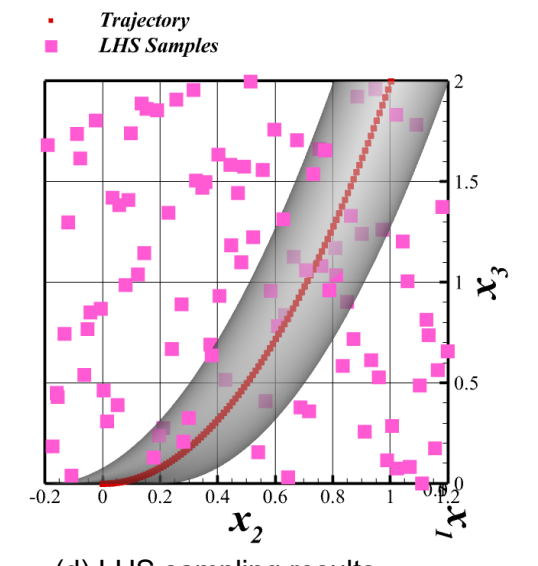




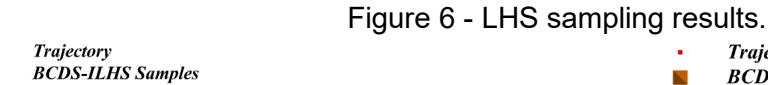
(c) LHS sampling results $x_1 - x_3$

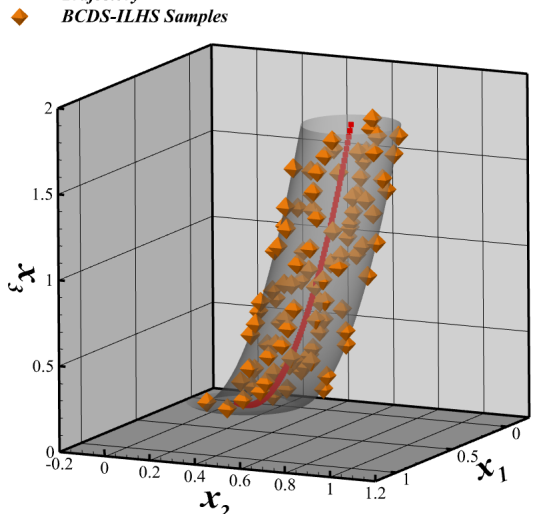


(b) LHS sampling results $x_1 - x_2$

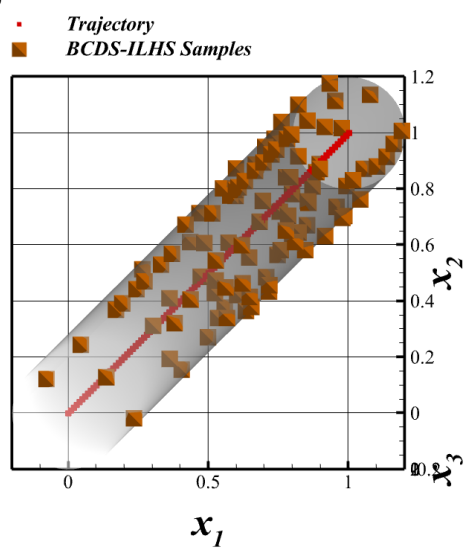


(d) LHS sampling results $x_2 - x_3$





(a) BCDS-ILHS sampling results $x_1 - x_2 - x_3$



(b) BCDS-ILHS sampling results $x_1 - x_2$

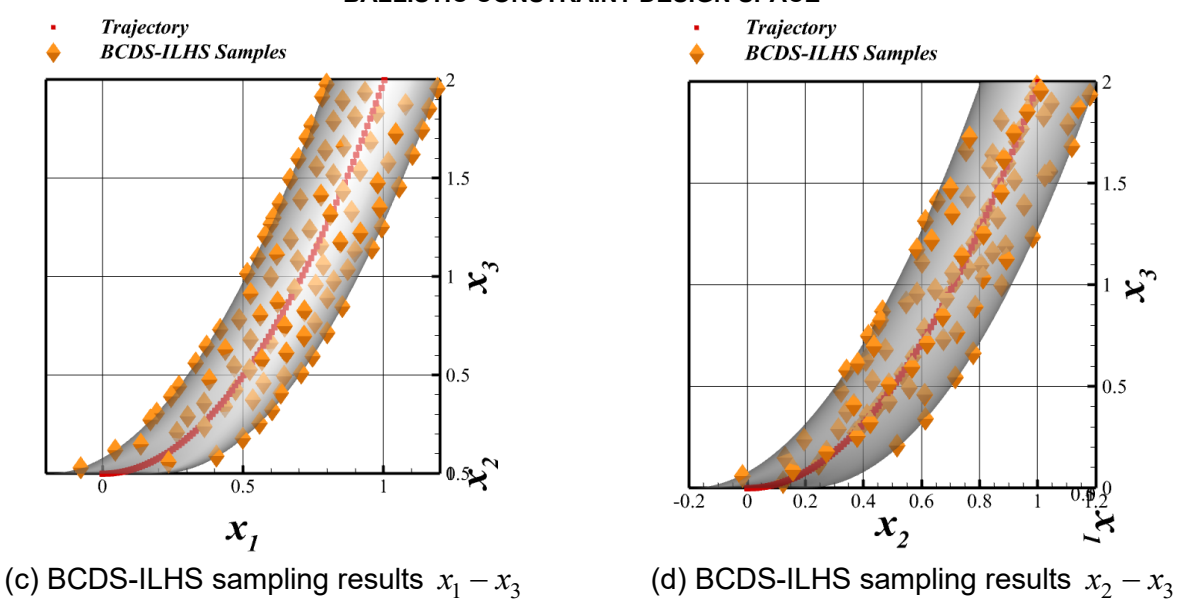


Figure 7 - BCDS-ILHS sampling results.

As can be seen in Figure 6 and Figure 7, most of the samples obtained by LHS do not satisfy the constraints, while all the samples obtained by BCDS-ILHS are strictly within the constraints.

In order to further test the feasibility of BCDS-ILHS for the DoE problem and modeling problem in the ballistic constraint design space, 10, 20, 30, 40 and 50 samples are taken as training samples by using LHS and BCDS-ILHS, respectively. And 101 samples are selected uniformly from the ballistic trajectory as test samples. The surrogate model uses Kriging. In the two sampling methods, f(x) of the three error metrics R^2 , RRMSE and RMAE with the increase of the number of training samples is shown in Figure 8. From the figure, it can be seen that all the error metrics of BCDS-ILHS are significantly better and more robust than LHS for different number of training samples. The feasibility of the proposed method in this paper is verified for the DoE problem and modeling problem in the ballistic constraint design space.

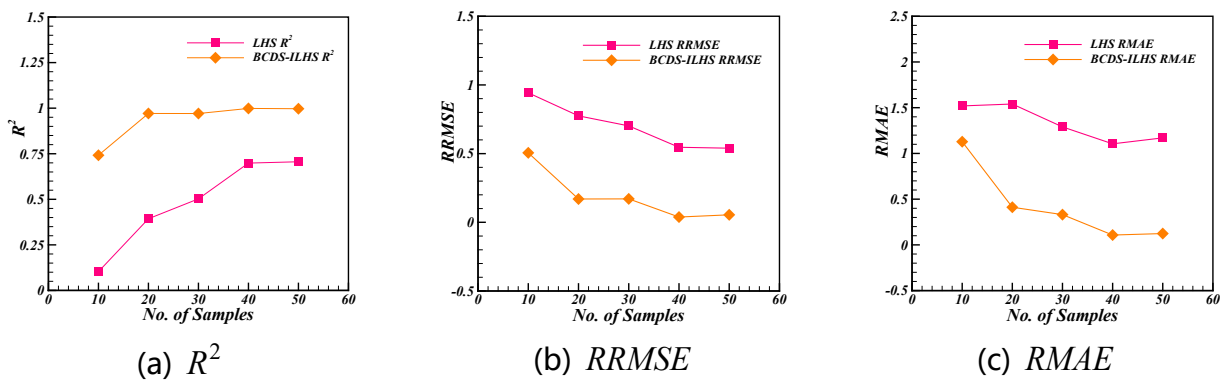


Figure 8 - Variation of the three error metrics \mathbb{R}^2 , $\mathbb{R}\mathbb{R}\mathbb{R}$ and $\mathbb{R}\mathbb{R}\mathbb{R}$ of \mathbb{R} with increasing number of training samples in the two sampling methods.

3.2 Case 2: Three-dimensional Engineering Case

The FDL-5A hypersonic vehicle (shown in Figure 2) is used to fly on the ballistic trajectory shown in Figure 9. Its C_L, C_D, C_M are used as the modeling targets. H, Ma, α are used as the variable. The DoE problem and the modeling problem in the ballistic constraint design space are simulated by

sampling and building Kriging for FDL-5A $\,C_L,C_D,C_M\,$. The design space is as follows

$$10.0511 \ km \le H \le 19.7947 \ km$$
$$5.65 \le Ma \le 15.22 \tag{17}$$

$$3.74^{\circ} \le \alpha \le 12.50^{\circ}$$

The ballistic constraints are established based on the following assumption: with H as the base dimension, for the sample to be collected $(H_x, Ma_a^{H_x}, \alpha_a^{H_x})$ at the height of H_x , the $Ma_a^{H_x}$ and $\alpha_a^{H_x}$ Euclidean distances of $Ma_0^{H_x}$ and $\alpha_0^{H_x}$ from the ballistic point $(H_x, Ma_0^{H_x}, \alpha_0^{H_x})$ at the height of H_x on the trajectory should not be greater than R. This assumption is mainly based on the fact that states on the trajectory usually do not mutate too much. Specifically, when H is changed from 11.0 km to 11.1 km, the Ma usually will not be mutate from 5.65 to 15.22. Therefore, the constraint equations for the ballistic trajectory are as follows

$$\sqrt{(Ma_a^{H_x} - Ma_0^{H_x})^2 + (\alpha_a^{H_x} - \alpha_0^{H_x})^2} \le R$$
(18)

where R is given as 1.0.

H is selected as the base dimension, and the BCDS-ILHS search steps in the Ma, α dimension are all

$$\lambda_{BCDS-ILHS} = 0.001 \tag{19}$$

The design space, ballistic trajectory and ballistic constraints are shown in Figure 9. When the value of H is determined, the ballistic constraints (blue circle) are shown in Figure 9 (a), and the complete ballistic constraints obtained from the ballistic trajectory are shown in Figure 9 (b) (gray pipe).

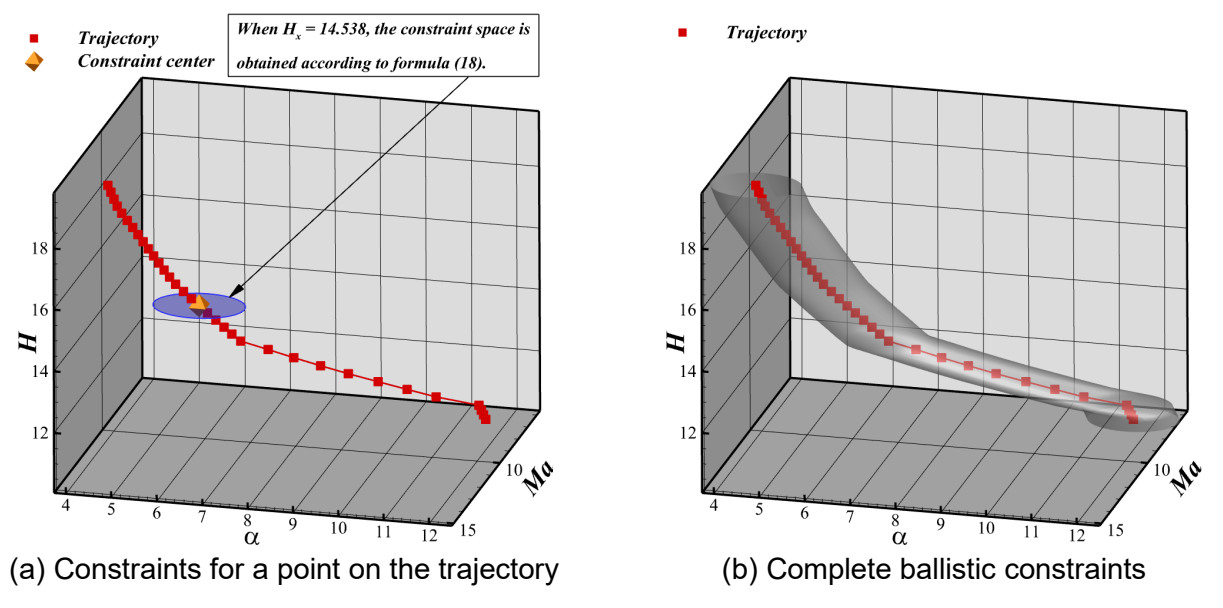
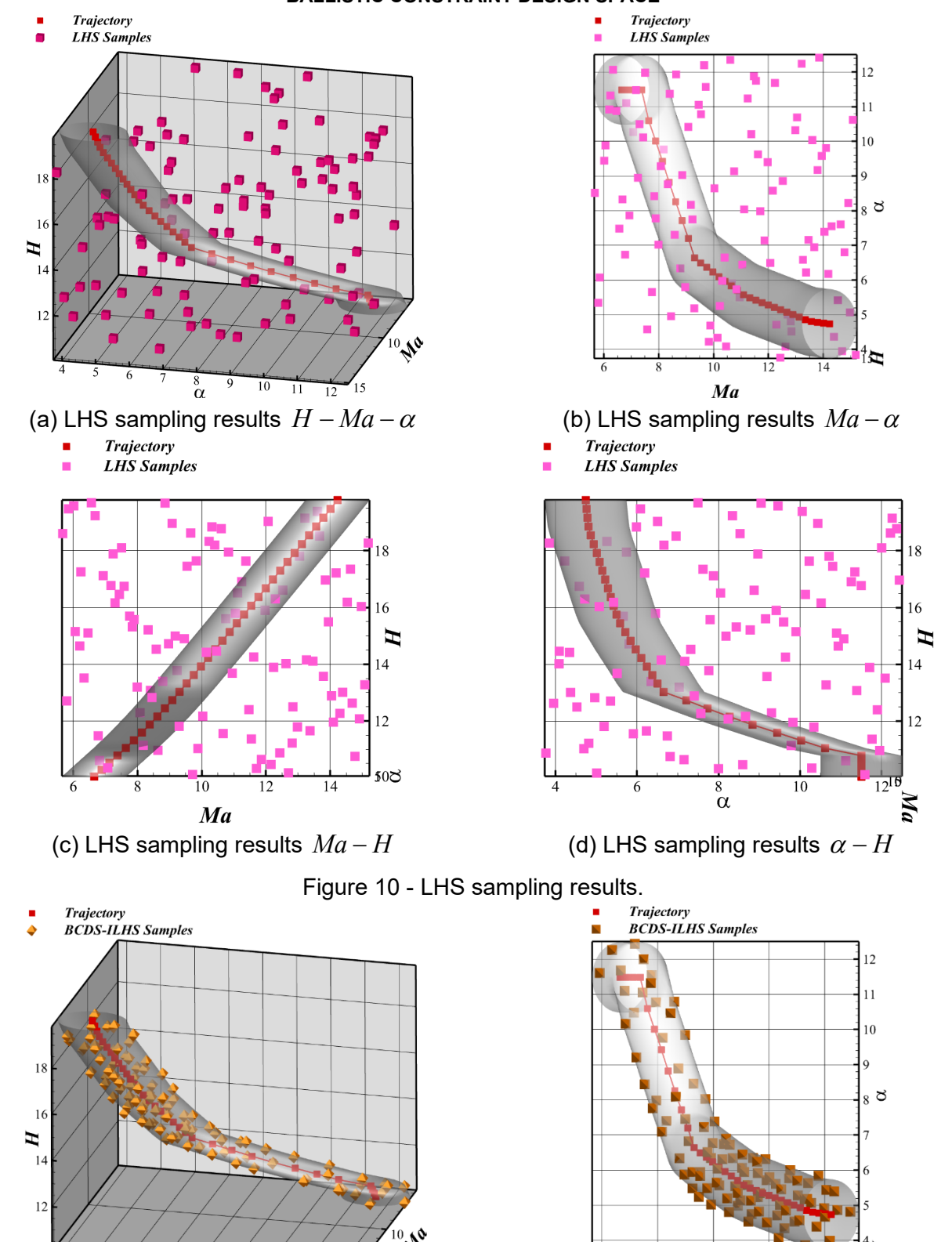


Figure 9 - FDL-5A design space, ballistic trajectory and ballistic constraints.

The LHS and BCDS-ILHS are used to sample the above design space with a sample size of 100, and the sampling results are shown in Figure 10 and Figure 11.



(b) BCDS-ILHS sampling results $Ma - \alpha$

(a) BCDS-ILHS sampling results $H-Ma-\alpha$

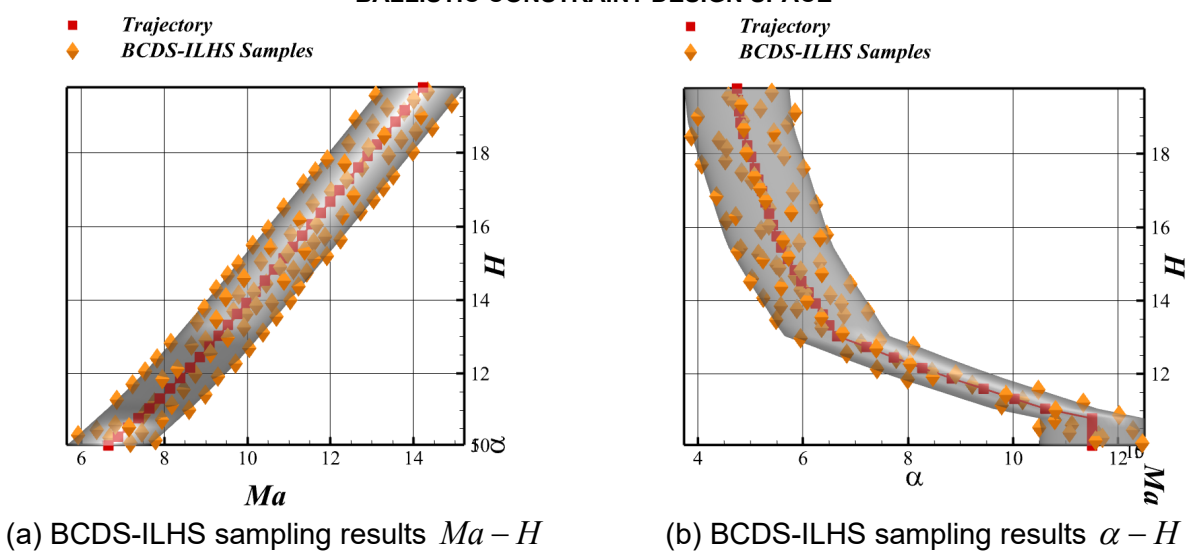


Figure 11 - BCDS-ILHS sampling results.

As can be seen in Figure 10 and Figure 11, most of the samples obtained through LHS do not satisfy the constraints, whereas all the samples obtained from BCDS-ILHS are strictly within the constraints.

In order to further test the feasibility of BCDS-ILHS for the DoE problem and modeling problem in the ballistic constraint design space, 5, 10, 15, 20 and 25 samples are taken as training samples using LHS and BCDS-ILHS, respectively. And 34 ballistic points on the ballistic trajectory are selected as test samples. The surrogate model uses Kriging. In order to reduce the computational cost, the mesh is chosen to be 48W (as shown in Figure 3 (a)), and the numerical simulation method is adopted as mentioned in Section 2.2. The variations of the three error metrics R^2 , RRMSE and RMAE of C_L , C_D , C_M with the increase of the number of training samples in both sampling methods are shown in Figure 12 to Figure 14. When the number of samples is small, in Figure 12 and Figure 14, although the BCDS-ILHS accuracy is slightly worse than the LHS, it is worth noting that both have achieved high accuracy. In Figure 13, the BCDS-ILHS accuracy is much larger than the LHS, and the LHS accuracy is poor. When the number of samples is large, the accuracy of the two methods gradually converges (as shown in Figure 12 to Figure 14). Initially, the feasibility of the method proposed in this paper is verified in the DoE problem and modelling problem in the ballistic constraint design space.

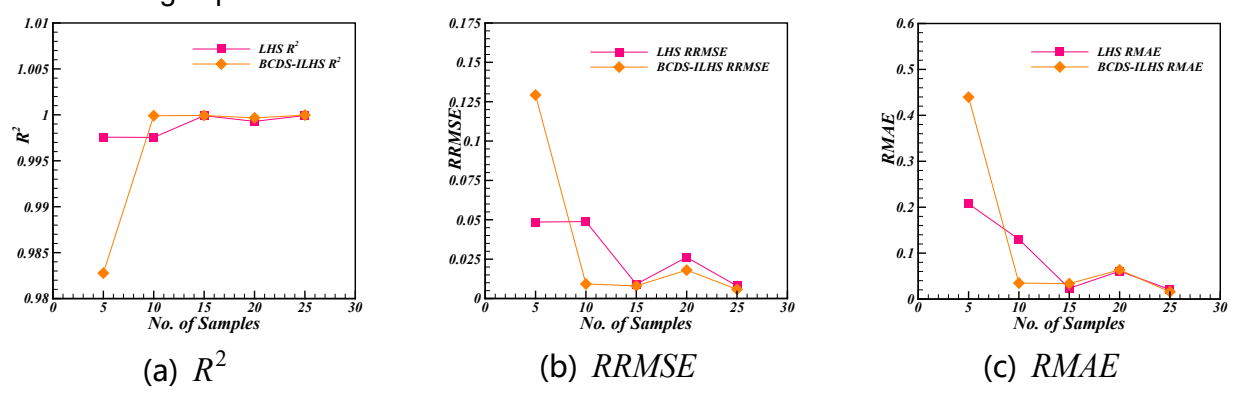


Figure 12 - Variation of the three error metrics \mathbb{R}^2 , \mathbb{R}^2 and \mathbb{R}^2 and \mathbb{R}^2 of \mathbb{R}^2 with increasing number of training samples in both sampling methods.

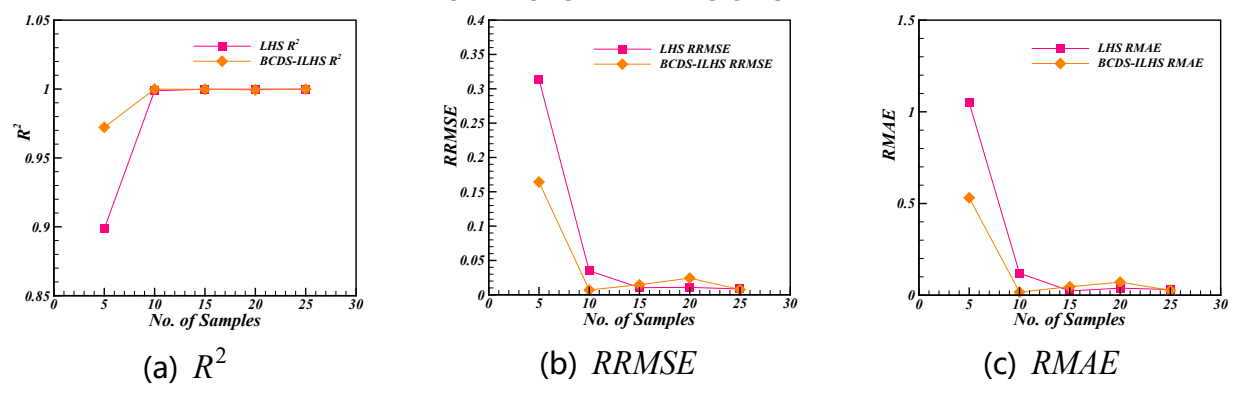


Figure 13 - Variation of the three error metrics \mathbb{R}^2 , \mathbb{R}^2 , \mathbb{R}^2 and \mathbb{R}^2 of \mathbb{R}^2 with increasing number of training samples in both sampling methods.

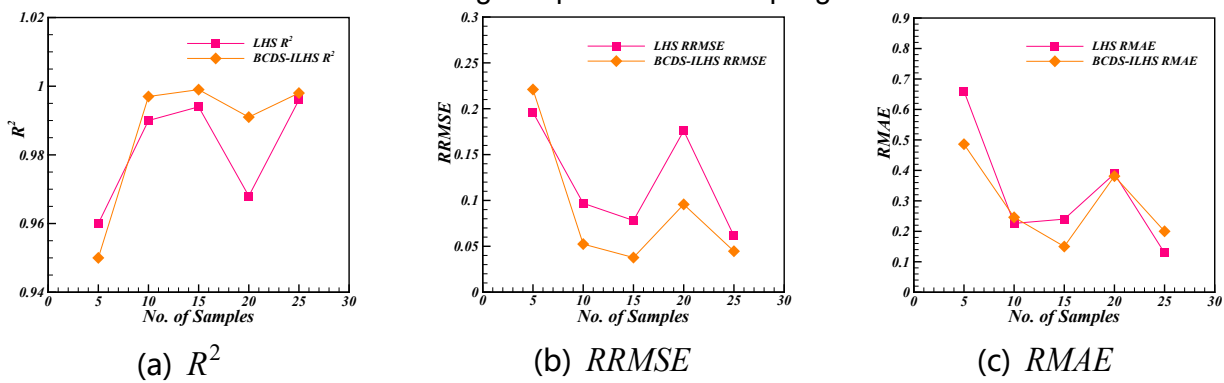


Figure 14 - Variation of the three error metrics \mathbb{R}^2 , \mathbb{R}^2 , \mathbb{R}^2 and \mathbb{R}^2 of \mathbb{R}^2 with increasing number of training samples in both sampling methods.

Combining the results of numerical and aerodynamic calculations, it can be seen that the method proposed in this paper is feasible for DoE problems and modelling problems in the ballistic constraint design space.

4. Conclusions

In this paper, a sequential local enumeration-based improved Latin hypercube sampling method for ballistic constraint design space is proposed, and the main conclusions are summarized as follows:

- (1) The constraints of the ballistic constraints design space are established based on the trajectory, which ensures a better exploration of the design space and improves the sampling correctness and accuracy under the condition that the samples strictly satisfy the constraints.
- (2) BCDS-ILHS is used in the DoE problem of ballistic constraint design space for a 3D numerical case and a 3D aerodynamic case. Compared with the sampling results of LHS, the results obtained from BCDS-ILHS sampling strictly satisfy the constraints, which proves the feasibility of the method proposed in this paper in the DoE problem of ballistic constraint design space.
- (3) BCDS-ILHS is used to model the ballistic constraint design space for a 3D numerical case and a 3D aerodynamic case. Comparison of the modelling results between the LHS and BCDS-ILHS samples shows that the latter requires fewer samples to build a more accurate surrogate model in most cases, which initially demonstrates the feasibility of the proposed method in the problem of modelling the ballistic constraint design space. However, it should be noted that the accuracy of

BCDS-ILHS is slightly worse than that of LHS for a small number of samples in the $\,C_D\,$ modelling of aerodynamic case, which may be related to the vehicle, design space and flow characteristics.

Although BCDS-ILHS is feasible in this paper, it is only a preliminary exploration. And Its applicability in high dimensional and complex ballistic constraint design space remains to be investigate. Also, regarding the ${\cal C}_D$ modelling problem mentioned in conclusion (3), it will be investigated in future work.

5. Acknowledgement

This research was sponsored by The Youth Innovation Team of Shaanxi Universities and The National Key Research and Development Program of China under Grant No. 2023YFB3002800.

6. Contact Author Email Address

Zhong-Hua Han: hanzh@nwpu.edu.cn

7. Copyright Statement

The authors confirm that they, and/or their company or organization, hold copyright on all of the original material included in this paper. The authors also confirm that they have obtained permission, from the copyright holder of any third party material included in this paper, to publish it as part of their paper. The authors confirm that they give permission, or have obtained permission from the copyright holder of this paper, for the publication and distribution of this paper as part of the ICAS proceedings or as individual off-prints from the proceedings.

References

- [1] Han Z H. Kriging surrogate model and its application to design optimization: a review of recent progress. *Acta Aeronautica et Astronautica Sinica*, Vol. 37, No. 11, pp 3197-3225, 2016.
- [2] Wang S, Lv L Y, Du L, et al. An improved LHS approach for constrained design space based on success -ive local enumeration algorithm. *Proceedings of 9th IEEE International Conference on CYBER Technolo -gy in Automation, Control, and Intelligent Systems,* Suzhou, China, pp 896-899, 2019.
- [3] Mckay M D, Beckman R J and Conover W J. A comparison of three methods for selecting values of input variables in the analysis of output from a computer code. *Technometrics*, Vol. 42, No. 1, pp 55-61, 2000.
- [4] Kalagnanam J R, Diwekar U M. An efficient sampling technique for off-line quality control. *Technometrics*, Vol. 39, No. 3, pp 308-319, 1997.
- [5] Owen A B. Orthogonal arrays for computer experiments, integration and visualization. *Statistica Sinica*, Vol. 2, No. 2, pp 439-452, 1992.
- [6] Wang Y, Fang K T. A note on uniform distribution and experimental design. *KEXUE TONGBAO*, Vol. 26, No. 6, pp 485-489, 1981.
- [7] Draper N R, Lin D K J. Small response-surface designs. *Technometrics*, Vol. 32, No. 2, pp 187-194, 199-0.
- [8] Liu F, Han Z H, Zhang Y, et al. Surrogate-based aerodynamic shape optimization of hypersonic flows considering transonic performance. *Aerospace Science and Technology*, Vol. 93, 2019.
- [9] Li J C, Cai J S. Massively multipoint aerodynamic shape design via surrogate-assisted gradient-based optimization. *AIAA JOURNAL*, Vol. 58, No. 5, pp 1949-1963, 2020.
- [10] Bailly J, Bailly D. Multifidelity aerodynamic optimization of a helicopter rotor blade. *AIAA JOURNAL*, Vol. 57, No. 8, pp 3132-3144, 2019.
- [11] Petelet M, Looss B, Asserin O, et al. Latin hypercube sampling with inequality constraints. *AStA Advanc* -es in Statistical Analysis, Vol. 94, pp 325-339, 2010.
- [12] Trosset M W. Approximate maxmin distance designs. *Proceedings of the Section on Physical and Engin -eering Sciences*, pp 223-227, 1999.
- [13] Stinstra E, Hertog D, Stehouwer P, et al. Constrained maximin designs for computer experiments. *Technometrics*, Vol. 45, No. 4, pp 340-346, 2003.
- [14] Draguljić D, Santner T J and Dean A M. Noncollapsing space-filling designs for bounded nonrectangular regions. *Technometrics*, Vol. 54, No. 2, pp 169-178, 2012.
- [15] Fuerle F, Sienz J. Formulation of the Audze–Eglais uniform Latin hypercube design of experiments for c -onstrained design spaces. *Advances in Engineering Software*, Vol. 42, pp 680-689, 2011.
- [16] Du L, Lv L Y, Sun W, et at. An Latin hypercube sampling approach for constrained design space. *Machinery Design & Manufacture*, No. 8, pp 43-47, 2021.
- [17] Ehrlich C F, Rising J J, Peyton R S, et al. Preliminary design and experimental investigation of the FDL-5A unmanned high L/D spacecraft. part 3. aerodynamics. *LOCKHEED-CALIFORNIA CO BURBANK*, 19-68.
- [18] Lyu Z J, Kenway G K W, Martins J R R A. Aerodynamic shape optimization investigations of the common research model wing benchmark. *AIAA JOURNAL*, Vol. 53, No. 4, pp 805-1117, 2015.
- [19] Krige D G. A statistical approach to some basic mine valuations problems on the witwatersrand. *Journal of the Chemical, Metallurgical and Mining Engineering Society of South Africa*, Vol. 52, No. 6, pp 119-13 -9, 1951.
- [20] Sacks J, Welch W J, Mitchell T J, et al. Design and analysis of computer experiments. *Statistical Scienc* -e, Vol. 4, No. 4, pp 409-423, 1989.